

Design and Simulation of Stand Alone Photovoltaic Systems

SALIMA KEBAILI¹, ACHOUR BETKA²

¹Department of Electrical Engineering
Oum El Bouaghi University
ALGERIA

salimakebaili@yahoo.fr

²Department of Electrical Engineering
Biskara University
ALGERIA

Abstract: - This paper presents the design and simulation of a stand alone photovoltaic system. The main activities of this work purpose to establish library mathematical models for each individual component of stand alone photovoltaic system. Control strategy has been considered to achieve permanent power supply to the load via photovoltaic/battery based on the power available from the sun. The complete model was simulated under two testing including sunny and cloudy conditions.

Key-Words: - Renewable energy, Photovoltaic system, Lead-acid battery, Modeling, Control, Simulation.

1 Introduction

Renewable energy sources are considered as alternative energy source to conventional fossil fuel energy sources due to environmental pollution and global warming and breaking of ozone barrier by exhausting carbon dioxide. To overcome this problem, photovoltaic system can integrate with other power generators or storage systems such as battery bank. The feasibility of photovoltaic system has been successfully demonstrated for both grid-connected and stand alone photovoltaic [1]. The stand alone photovoltaic (SAPV) now represent only 8.4% of the total photovoltaic installed power amount in IEA PVPS countries, the electrification of areas, notably rural areas, by SAPV systems must be taken into account [2]. Various aspect must be taken into account when working with SAPV system for the generation of electricity. Reliability and cost are two aspects of these aspects; it's possible to confirm that SAPV are economically viable, especially in remote locations. In addition, climate can make one type more profitable than another type. For example, SAPV systems are ideal in areas with warm climates.

On the other hand, various mathematical models of the element that make up this system have been used, as well, as various design and simulation models. The complexity of the models of the components of the SAPV systems mainly depends on the type of application [3].

The main aim of this paper is to establish a library models for each individual components of stand alone systems. Design and control strategy has been developed and simulations have been performed in order to supply electricity to a DC loads. For this, the paper will be organized as follows. Section2 is devoted to present the studied system and treats the modeling of each components of SAPV system. The simulation results are presented in section3. Finally, conclusions are given in the last section.

2 Modeling of SAPV System

Figure1 represents an SAPV system. Firstly, the electricity production is provided photovoltaic module such a production depends directly on the solar irradiance profile. A maximum power point tracker (MPPT) is used in order to ensure optimal production, whatever the weather via the DC/DC converter. Secondly, the storage element which is unavoidable due to the inadequacy between the electricity photovoltaic production profile and the load profile is connected to the DC bus. Presently, due to its technical maturity and its economical cost, the storage system universally used is the lead-acid technology with a controller. Thirdly, DC loads are linked with the DC bus. Finally, for protection, shunt resistance and several switches are used. The part of grid connected to the system is not included.

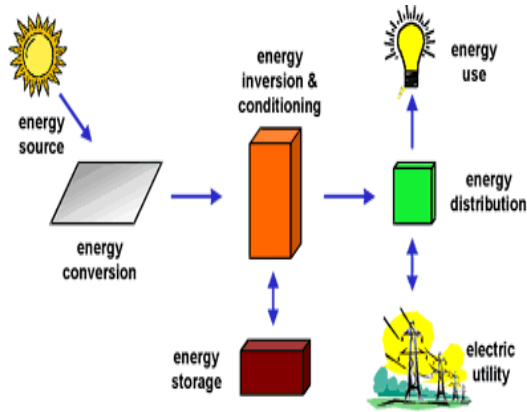


Fig.1 The studied system.

2.1 Modeling of photovoltaic module

To investigate current-voltage characteristics of photovoltaic array and maximum power point location for certain parameters variations, a simple photovoltaic module electrical model is designed based on the Shockley diode equation. A photovoltaic module, namely BPSX150 which contains 72 cells, is selected for the purpose of this research.

A photovoltaic cell is usually represented by an electrical equivalent one diode model [4],[5],[6] as shown in figure2.

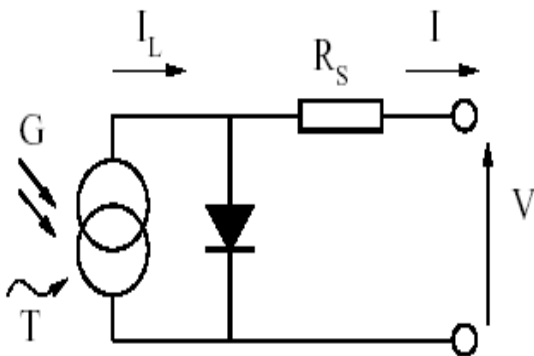


Fig.2 Model of photovoltaic cell.

The model contains a current source \$I_L\$, one diode and a series resistance \$R_s\$, which represents the resistance inside each cell and in the connection between the cells.

The output current from the photovoltaic cell can be found using the following equation:

$$I = I_L - I_D \tag{1}$$

Where \$I_L\$ is the photon generated current and \$I_D\$ is the current shunted through the intrinsic diode.

The diode current is given by the Shockley's diode equation:

$$I_D = I_0 (e^{q(V+IR_s)/n.T.k} - 1) \tag{2}$$

The reverse saturation current \$I_0\$, is dependent of temperature, and is described in this equation:

$$I_0 = I_0(T_{ref}) \cdot \left(\frac{T}{T_{ref}}\right)^{3/n} \cdot e^{-qV_g/n.k \cdot \left(\frac{1}{T} - \frac{1}{T_{ref}}\right)} \tag{3}$$

With

\$T\$: The junction temperature in Kelvin (K).

\$T_{ref}\$: The reference temperature of the PV cell in Kelvin, usually 298K.

\$n\$: Diode ideality factor (\$1 < n < 2\$)

\$q\$: Electron charge

\$k\$: Boltzmann's constant.

\$V_g\$: Gap voltage (V).

\$I_0(T_{ref})\$: is the reverse saturation current of the diode at the reference temperature is given by:

$$I_0(T_{ref}) = \frac{I_{sc}(T_{ref})}{(e^{qV_{oc}(T_{ref})/nkT_{ref}} - 1)} \tag{4}$$

The photo current \$I_L\$, can be calculated at a given temperature using:

$$I_L = I_L(T_{ref})(1 + k_0(T - T_{ref})) \tag{5}$$

With \$k_0\$ is the temperature coefficient of \$I_{sc}\$ percent change per degree temperature (found in the date sheet), since the value of the photon generated current can be assumed to be directly proportional to the irradiance, and the short circuit current is given under standard test conditions (\$G_0=1000W/m^2\$, \$T_{ref}=298K\$). Therefore, the photon generated current at any other irradiance, \$G(w/m^2)\$, is given by:

$$I_L(T_{ref}) = \frac{G}{G_0} \cdot I_{sc}(T_{ref}) \tag{6}$$

Hence, all constant values that taken from the data sheet of BPSX150, as shown in table 1, is used to carry out the simulation. Rated irradiance at standard test condition is 1000W/m², which equal to 1 sun at irradiance spectrum A.M 1.5 and at temperature, T of 25⁰C, while I_{sc}=4.75A and V_{oc}=43.5V.

An estimate must be made of the unknown 'ideality factor', it's takes a value between one and two, being near one at high current , rising towards two at low current. A value of 1.6 suggested as typical in normal operation. The effect of varying the ideality factor can be seen in figure 3.

Electrical Characteristics	BPSX150
Maximum power	150W
Voltage at max. power	34.5V
Current at max. power	4.35A
Short circuit current	4.75A
Open circuit voltage	43.5V
Temp.coefficient of I _{sc}	(0.065+.015)%/ ⁰ C
Temp. coefficient of V _{oc}	-(160+20)mV/ ⁰ C
Temp. coefficient of power	-(0.5+.05)%/ ⁰ C

Table 1 The key specifications of the BPSX150.

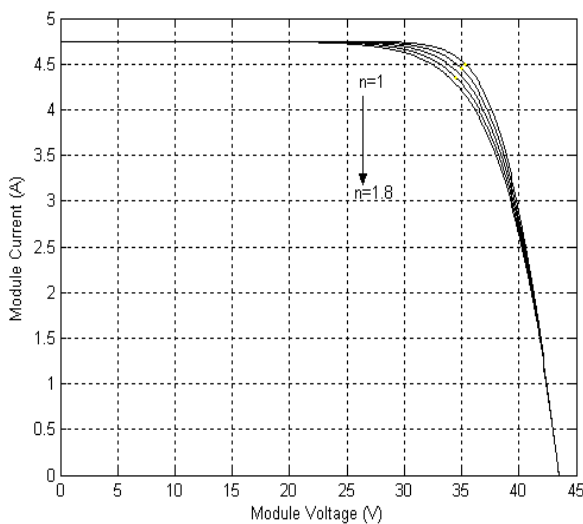


Fig.3 V-I Characteristic for various diode ideality factors.

By differentiating equation (1), evaluating at V=V_{oc} and rearranging terms of R_s, we found:

$$R_s = -\frac{dV}{dI} - \frac{1}{X_V} \tag{7}$$

With,

$$X_V = I_0(T_{ref}) \cdot \frac{q}{nkT_{ref}} \cdot e^{\frac{qV_{oc}(T_{ref})}{nkT_{ref}}} \tag{8}$$

The series resistances of the panel has a large impact on the slope of I-V curve at V=V_{oc}, as seen in figure 4. Using the values obtained from the BPSX150 manufactures curves, a value of series resistance R_s=5.1mΩ was calculated.

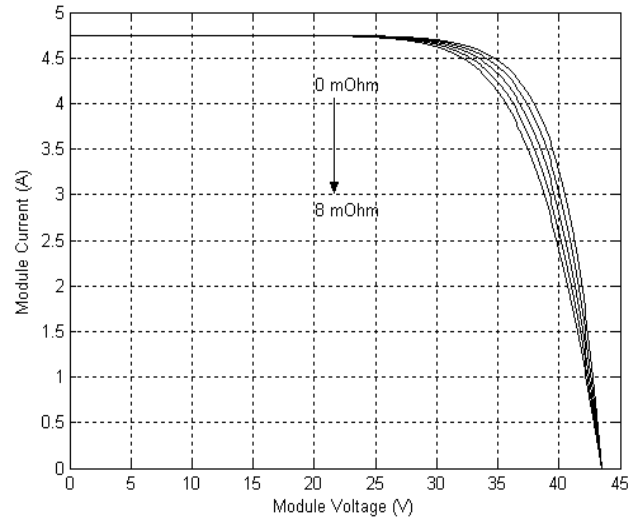


Fig.4 V-I Characteristic for various model series resistances.

2.2 MPPT control algorithm

As known the output power characteristics of a solar panel, there is an optimum operating point (MPP) such that the PV delivers the maximum possible power to the load. The optimum operating point changes with the solar irradiation and cell temperature are shown in figure 5 and figure 6 respectively. Therefore, on line tacking of the maximum power point (MPPT) of a PV array is an essential part of any successful PV system. A variety of maximum power points tracking methods are developed. The methods vary in implementation complexity, sensed parameters, required number of sensors, convergence speed and cost [7]. There are many MPPT available in the literature [8-11]. The most widely used techniques are:

- Constant voltage method
- Short current pulse method
- Perturb & Observe method
- Incremental conductance method

In this paper, the incremental conductance method is applied. The heart of MPPT hardware is a switch mode DC/DC converter which must be inserted between the solar panel and the battery.

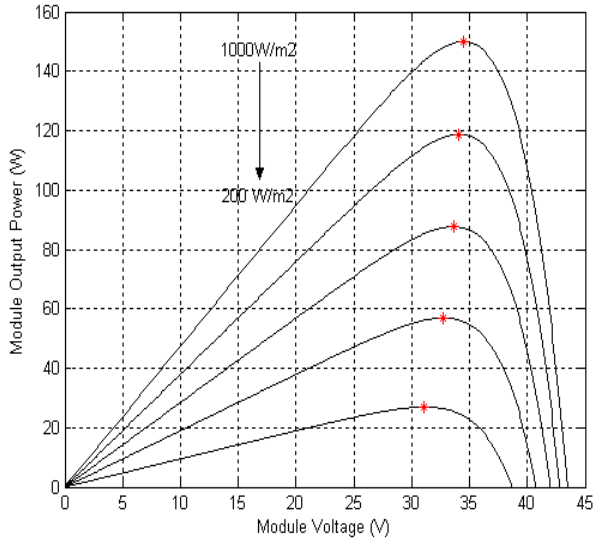


Fig.5 Output power characteristics at various irradiances.

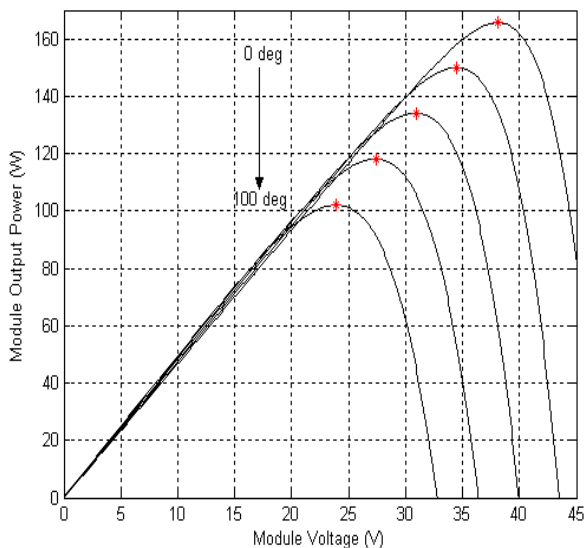


Fig.6 Output power characteristics at various temperatures.

2.2.1 Incremental conductance method

The incremental conductance algorithm is derived by differentiating the PV array power with respect to voltage and setting the result equal to zero [12]

$$\frac{dP}{dV} = I + V \frac{dI}{dV} = 0 \text{ at the MPP} \tag{9}$$

Rearranging equation (9) gives:

$$\frac{dI}{dV} = -\frac{I}{V} \tag{10}$$

If the operating point is the left side of the MPP:

$$\frac{dI}{dV} > -\frac{I}{V} \tag{11}$$

If the operating point is the right side of the MPP:

$$\frac{dI}{dV} < -\frac{I}{V} \tag{12}$$

Note that the left side of the Eqns.10-12 represents incremental conductance of the PV module and the right side of the equation represents its instantaneous conductance. The incremental conductance algorithm starts with measuring the present values of PV module voltage and current. Then, it calculates the incremental changes, dI and dV, using the present values of voltage and current. The main check is carried out by comparing $\frac{dI}{dV}$ against $(-\frac{I}{V})$, and according to the results of this check, the control reference signal V_{ref} will be adjusted in order to move the array terminal voltage towards the MPP voltage. When the above incremental was tested, we noted that the condition $(\frac{dP}{dV}=0)$ seldom occurred because of the approximation made in the calculation of dI and dV. However, this condition can be detected by allowing a small marginal error (E) in the above comparison $(\frac{dP}{dV}=\pm E)$ and the value of E depends on the required sensitivity of MPP [13].

2.3 DC/DC converter

There are a number of different topologies for DC/DC converter. They are categorized into isolated or non-isolated topologies.

The isolated topologies use a small sized high frequency electrical isolation transformer which provides the benefits of DC isolation between input and output, step-up or down of output voltage by changing the transformer turns ratio but the non-isolated topologies do not have isolation transformer.

In our design we adopted a Cuk converter. It's a type of the second category. It can provide the

output voltage that is higher or lower than the input voltage and on the other hand, the input current of the Cuk converter is continuous and they can draw a ripple free current from a PV array that is important for efficient MPPT. Fig.7 shows a circuit diagram of the basic Cuk converter. It can provide a better output current characteristic due to the inductor on the output stage.

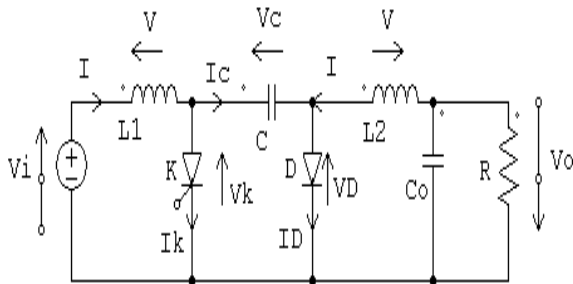


Fig.7 Circuit diagram of the basic Cuk converter.

The output voltage is given by:

$$V_o = V_i \left(\frac{D}{1-D} \right) \quad (13)$$

Where, D is the duty cycle.

The input impedance of the converter is described by the following equation:

$$R_{in} = \left(\frac{1-D}{D} \right)^2 \cdot R_{load} \quad (14)$$

The impedance seen by PV is the input impedance of the converter. By changing the duty cycle, the value R_{in} can be matched with that of optimum load, which is defined by the coordinates of the MPP [12-14].

$$R_{opt} = \frac{V_{MPP}}{I_{MPP}} \quad (15)$$

We can calculate the value of α that matches the load to the PV array as a function of the atmospheric condition, as shown in Fig. 8.

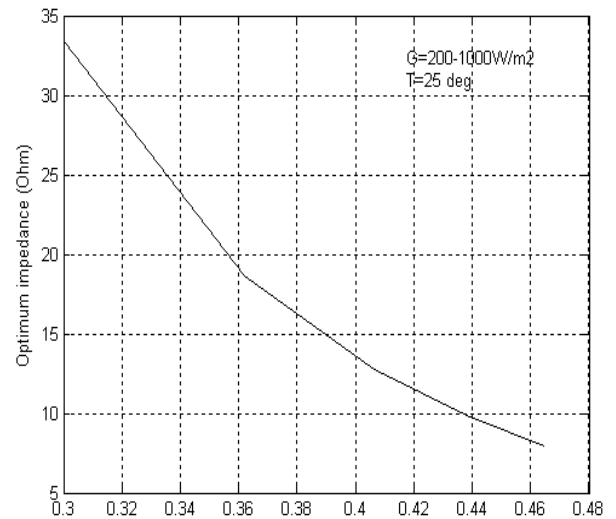


Fig.8 Duty ratio to match a fixed load to the PV array.

2.4 Storage

The battery is necessary in such a system because of the fluctuating nature of the output delivered by the PV arrays. Thus, during the hours of sunshine, the PV system is directly feeding the load, the excess electrical energy being stored in the battery. During the night, or during a period of low solar irradiation, energy is supplied to the load from the battery. Therefore, we need to use electrical modelling of the storage element. The models of the lead-acid batteries are widely used in PV application. In fact a large number of models exist in literature [15-19]. The accumulator is modelled by two electrical non linear elements: a voltage source representing the open-circuit voltage (V_1) of the accumulator, and an internal resistance (R_1) for the different losses, as shown in Fig.9.

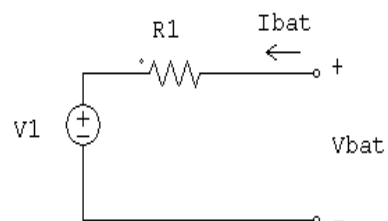


Fig.9 Lead-acid accumulator modeling.

The terminal voltage of the battery, V_{bat} is given by:

$$V_{bat} = V_1 \pm R_1 \cdot I_{bat} \quad (16)$$

This model develops different equations for charging and discharging. This is basically the energy balance equation computing the value of the state of charge (soc) increment as the energy increment in a differential of time taking into account self-discharge (α) and charge and discharge efficiency (k).

The electrical equations of the accumulator for charging and discharging are quoted below:

Charge mode:

$$V_1 = [2 + 0.148 \cdot \text{soc}(t)] n_s \quad (17)$$

$$R_1 = \frac{0.758 + 0.1309/[1.06 - \text{soc}(t)] n_s}{\text{soc}_m} \quad (18)$$

Discharge mode:

$$V_1 = [1.926 + 0.124 \cdot \text{soc}(t)] n_s \quad (19)$$

$$R_1 = \frac{0.19 + 0.1037/[\text{soc}(t) - 0.14] n_s}{\text{soc}_m} \quad (20)$$

Where:

n_s : Number of cells in series

$\text{soc}(t)$: The current state of charge (%)

soc_m : Maximum battery capacity (Wh).

The most difficult part of the battery model is accurately estimating a value of state of charge. The estimation of this value is given by:

$$\text{soc}(t) = \text{soc}(t-1) + \int_{t-1}^t \frac{k \cdot V_1 \cdot I_{bat}}{60 \cdot \text{soc}_m} - \frac{\alpha \cdot \text{soc}(t-1)}{60} dt \quad (21)$$

Therefore $\text{soc}(t)$ can be found if you know the previous condition.

In order to prevent over-discharge and to limit gassing process [20], the soc is held in a limited range:

$$\text{soc}_{\min} < \text{soc} < \text{soc}_{\max} \quad (22)$$

With $\text{soc}_{\min}=0.3$ and $\text{soc}_{\max}=0.9$.

While the battery is charging, internal resistance still depends on the state of charge of the electrochemical accumulator. This value rises at an increasing rate when approaching the fully charged state. For illustration, figure 10 and figure 11 displays the evolution in internal resistance for our accumulator which is composed of six elements in series during both the charge and discharge regimes.

2.5 Controller

All power systems must include a control strategy that describes the interactions between its components. The use of battery as a storage form implies thus the presence of a charge controller.

The charge controller is used to manage the energy flow to PV system, batteries and loads by collecting information on the battery voltage and knowing the minimum (V_{\min}) and maximum (V_{\max}) values acceptable for the battery voltage. It consists of two switches. The first switch, on the PV module side, is opened if the battery voltage becomes larger than V_{\max} and will remain open until the battery voltage has dropped to critical voltage. The second switch, on the load side, is opened if the battery voltage drops below V_{\min} and remain in that state until the voltage has rebounded to critical voltage.

To protect the battery against the extra current when the battery is fully charged, a small resistance and a switch that is open unless the battery is fully charged and the PV module is delivering current.

The state of switches: State of open switch=0 and state of closed switch=1.

The block diagram for the studied system is shown in figure 12.

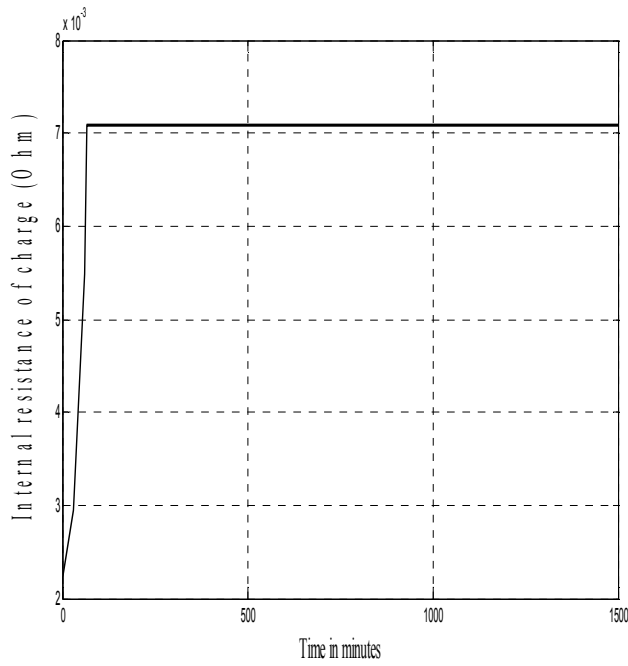


Fig.10 Evolution in the internal resistance of the battery in charge mode.

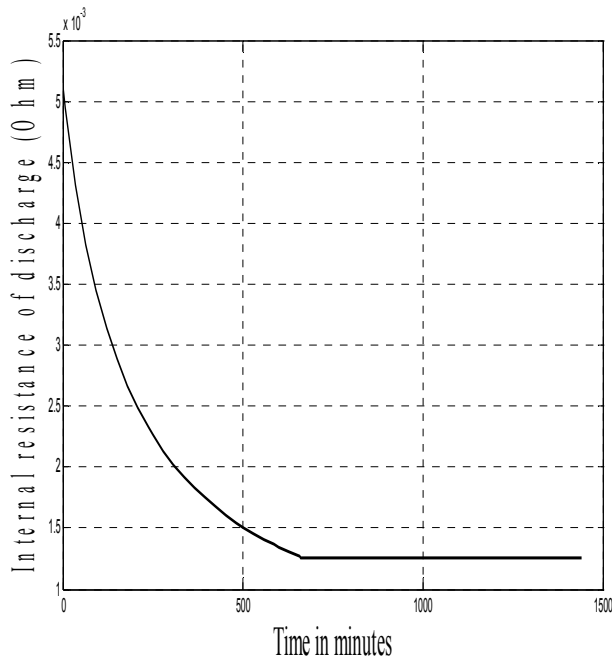


Fig.11 Evolution in the internal resistance of the battery in discharge mode

The block controlling the switches can be seen in figure 13. The battery voltage is passed through several compare to constant blocks, which output 1 if the condition is true and 0 if the condition is false. Those values are then entered into truth table along with the previous condition of the switch.

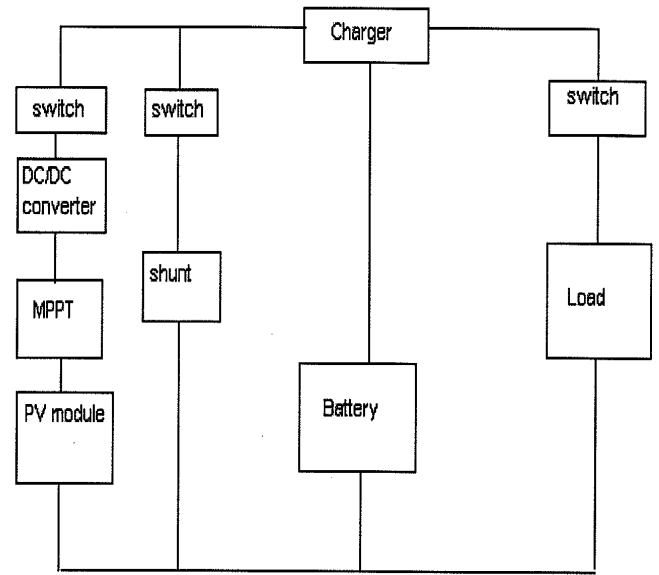


Fig.12 Block diagram for the studied system.

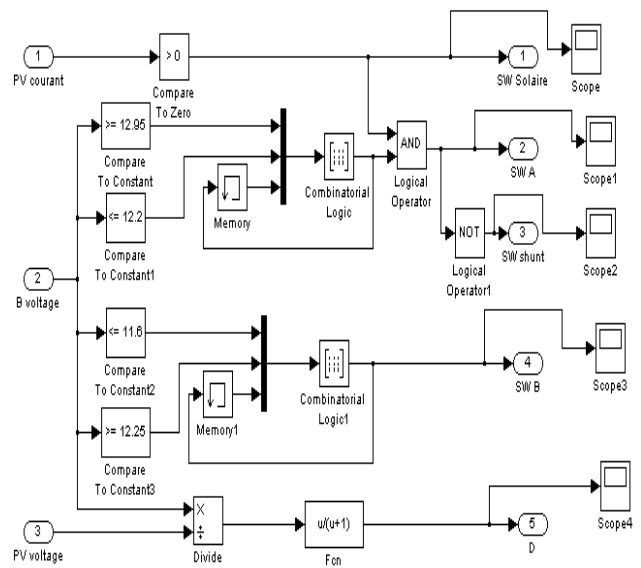


Fig.13 Controller model.

3 Simulation

In order to simulate the stand alone photovoltaic system, the daily solar irradiation has abrupt variations during the day for both sunny day and cloudy day is shown in figure 14 and figure 15.

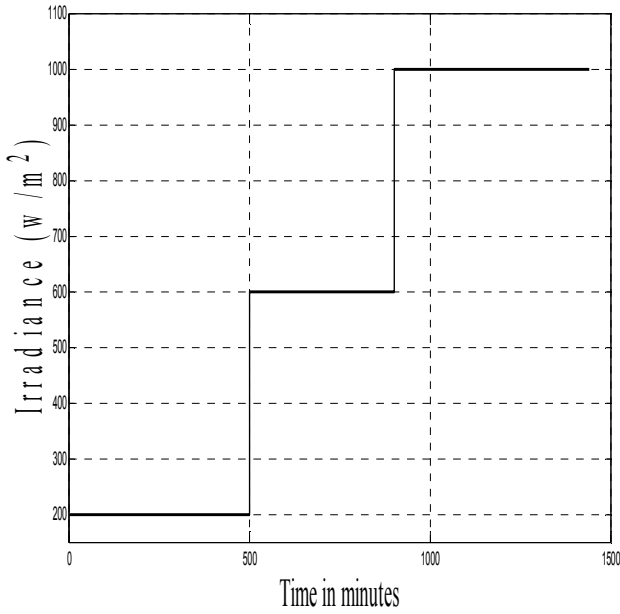


Fig.14 Daily solar irradiation diagram for sunny day

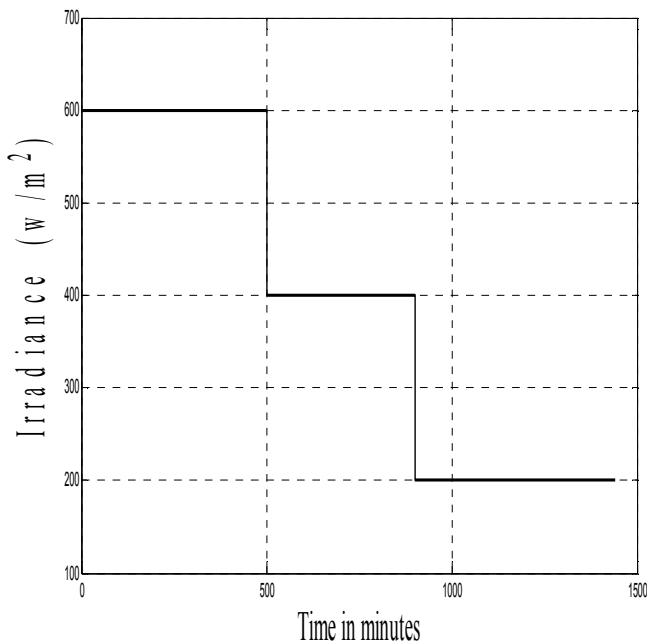


Fig.15 Daily solar irradiation diagram for cloudy day.

For the sunny day as shown in figure 14, the irradiation is increasing, the state of charge and battery voltage are increased. After the battery's charging, the voltage becomes equal to 12.84 Volts (for six cells in series) and soc approaches to 0.9. When the soc reaches this value, the battery is therefore charged as illustrated in figure 16.

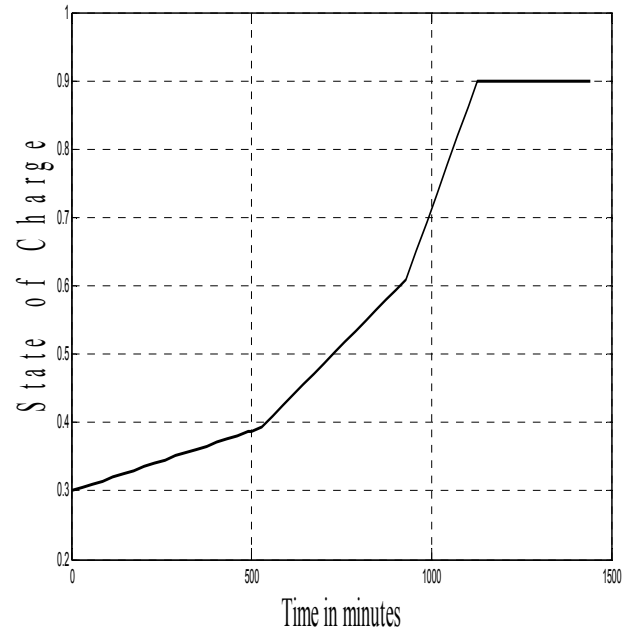
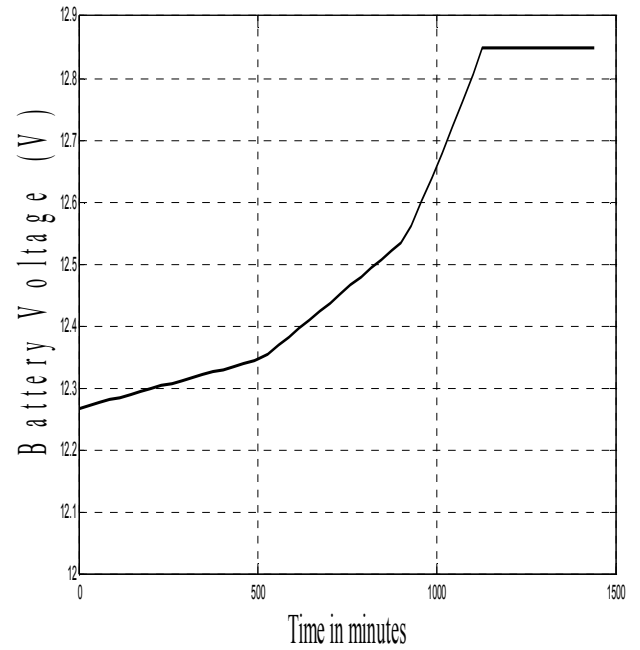


Fig.16 Battery Voltage and State of Charge.

3.1 Battery Charging

In order to test the charging state, the battery is connected to the solar model. The current entering the battery should be controlled.

3.2 Stand Alone Photovoltaic System

In this part, the controller must be used in order to control the flow of energy between different components of SAPV system.

Some constraints and initial conditions in our system must take:

1. Battery limits: In order to prevent overdischarge and to limit gassing process, the soc is held in a limited range: $0.3 < \text{soc} < 0.9$

The battery voltage must be lies between: $12.95 \text{ V} < V_{\text{bat}} < 11.6 \text{ V}$

2. Voltage condition: The voltage of the solar model must be greater than the voltage of the battery (for $n_s=6$, $V_{\text{bat}}=12 \text{ V}$).

3. Environmental conditions: The inputs of the solar model are: solar irradiation and temperature for both sunny day and cloudy day.

In order to validate the controller design incorporated in the SAPV system, a test for both the sunny day and cloudy day is applied.

During the day, the environmental conditions change, the controller plays the role in the energy management between the different blocs (photovoltaic module, battery and load).

For the sunny day, the PV module is directly used in the charging of the battery in their voltage limits, the state switch in side the PV module is close but the load is not connected, the state switch in side the load is open, as illustrated in figure 17. When the load is connected, this one requires a current produced by the battery.

Against, for the cloudy day, the load is connected and the battery is discharging, the state switch in side the load is close, as shown in figure 18. When the batteries reach the minimum allowable charging level and the load exceeds the power produced by the PV module, a supplementary source that will be able to be a fuel cell system takes over to supply the load and it can also function as an emergency generator if the PV generator system fails.

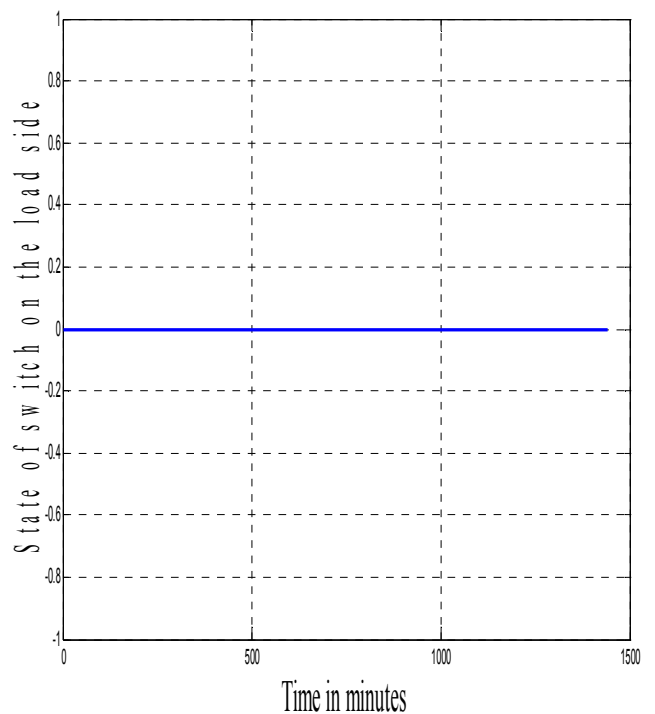
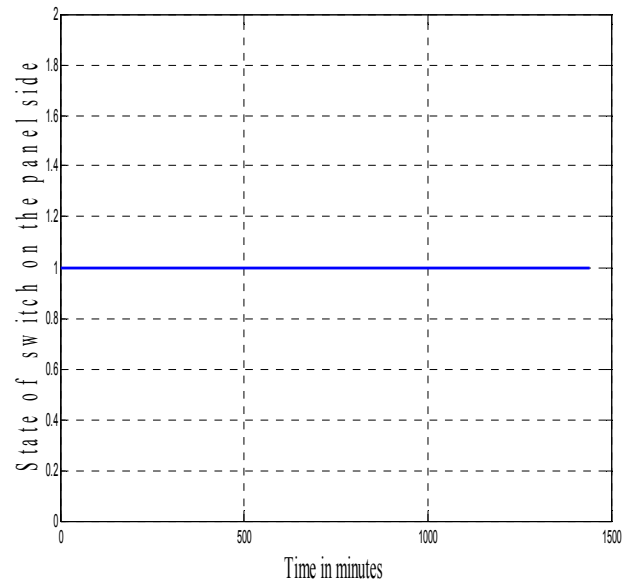


Fig.17 Sunny day: State switches in side the PV and the load.

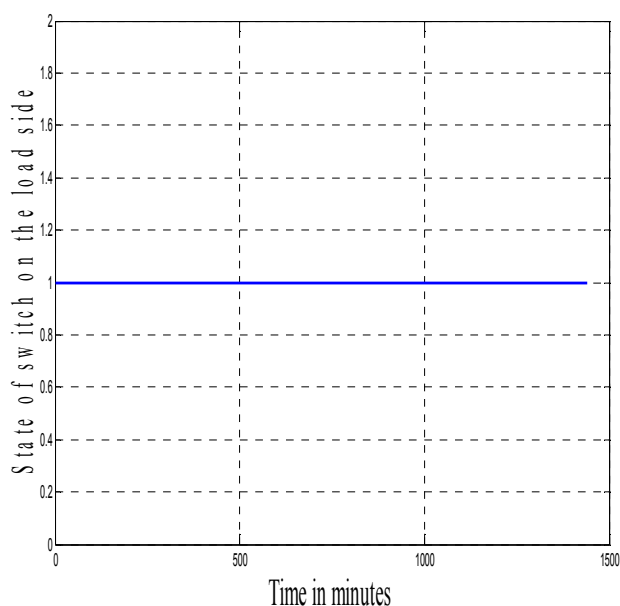
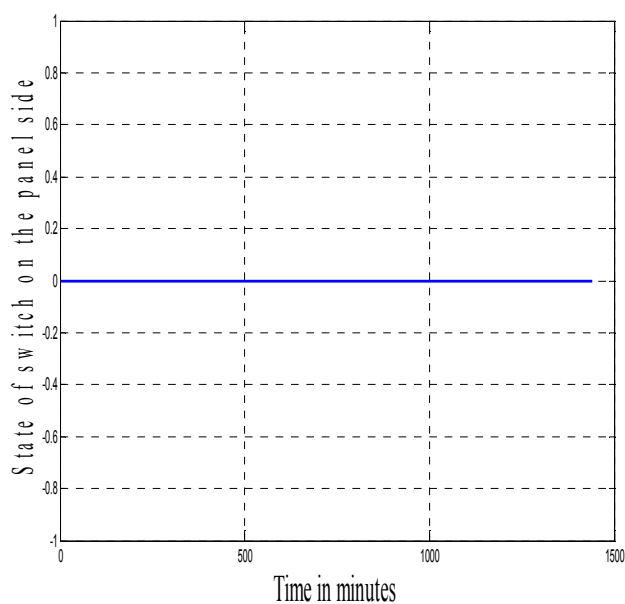


Fig.18 Cloudy day: State switches in side the PV and the load.

4 Conclusion

This paper has focused on the modeling of stand alone photovoltaic system. The model of a PV module connected to a lead acid battery was presented. Simulation results are analyzed and

validate the proposed model. Then, the stand alone photovoltaic system was treated. An efficient controller was placed in order to manage the energy flow to PV module, battery and loads. It gives a good strategy for the system functioning in the both sunny day and cloudy day. A model using 'Simulink-Matlab' software, which is a high level language and interactive environment, enables the prediction of the system intensive tasks in a fast and precise manner.

References:

- [1] Michael M.D.Ross, A Simple but Comprehension Lead Acide Battery Model for Hybrid System Simulation, *OP- J_411-Hybnd*, 2002.
- [2] Y.Thiaux, J.Seigneurbieux, B.Multon, H.Ben Ahmed, Load profile impact on the gross energy requirement of stand alone photovoltaic systems, *Renewable Energy*, Vol.35, 2010, pp.602-613.
- [3] D. Saheb-Koussa, M. Haddadi, M. Belhani, Economic and Technical study of a Hybrid System (Wind-Photovoltaic-Diesel) for Rural Electrification in Algeria, *Applied Energy*, Vol.86, 2009, pp. 1024-1030.
- [4] Walker.Geoff, Evaluating MPPT converter topologies using a Matlab PV model,
- [5] S.Kebaili,A.Betka, Efficiency model of DC/DC PWM converter photovoltaic applications, *2nd Conference International on Renewable Energy Approaches for Desert Regions and Exhibition*, 2009, 31 March- 02April, Amman, Jordan.
- [6] Y.Yusof,S.H.Sayuti,M.A.Latif,M.Z.C.Wanik, Modeling and simulation of maximum power point tracker for photovoltaic system, *National power& Energy Conference*,2004,pp.88-93.
- [7] Azab.Mohamed, A new maximum power point tracker for photovoltaic systems, *Proceeding of World Academy of Science Engineering and Technology*, Vol.35, 2008, pp.571-574.
- [8] Hohm.P, Rapp.M.E, Comparative study of maximum power point tracking algorithms, *Prog.Photovolt.Res.Appl*, Vol.11, 2002, pp.47-62.
- [9] Husein .K.Muta.I, Hoshina.T, Osakada.M, Maximum photovoltaic power tracking: an algorithm for rapidly changing atmospheric conditions, *IEE.Proc.Gener. Transm.Distrib* , Vol.142,1995,pp.59-64
- [10] Roberto.Faranda, Sonia.Leva, Energy comparison of MPPT techniques for PV

- systems, *WSEAS Transaction on Power Systems*, Vol.3, 2008, pp.446-455.
- [11] Sachin.Jain, Vivek.Agarwal, New current control based MPPT technique for single stage grid connected V systems, *Energy Conversion and Management*, 2006, pp.20-30.
- [12] Oi.Akihiro, Design and simulation of photovoltaic water pumping system, *Master's thesis, California Polytechnique State University*, 2005.
- [13] Tyson.Denherder, Design and simulation of photovoltaic super system using Simulink, *Master's thesis, California Polytechnique State University*, 2006.
- [14] Ionel. Laurentiu Alberteanu, Sergiu Ivanov, Gheorghe Manolea, Modeling and simulation of stand-alone photovoltaic system, *8th WSEAS Conference on Power Systems*, 2008, pp.189-194.
- [15] N. Moubayed, A. Eli-Ali , R. Outbib, Control of an Hybrid Solar-Wind System With Acid Battery for Storage, *WSEAS Trans. On Power Systems*, Vol.4, 2009, pp.307-318.
- [16] O.Gegaud, G. Robin, B.Multon, H.Ben.Ahmed, Energy modelling of a lead acid battery within hybrid wind/photovoltaic systems, *EPE*, 2003, pp1-10
- [17] N. Achaibou, M. Haddadi, A. Malek, Lead Acid Batteries Simulation Including Experimental Validation, *Journal of Power Sources*, Vol.185, 2008, pp.1484-1491.
- [18] A.Jossen, J.Garche, D.Urwe, Operation conditions of batteries in PV applications, *Solar Energy*, Vol.76, 2004, pp.759-769.
- [19] Jose.L, Bernal.Agustin, Rodolfo .Dufo .Lopez, Simulation and optimization of stand alone hybrid renewable energy systems, *Renewable and Sustainable Energy Reviews*, Vol.13, 2009, pp.2111-2118.
- [20] Abderrazak. Hammouche, Marc.Thele, Dirk.Uwe.Sauer, Analysis of gassing processes in a VRLA/spiral wound battery, *journal of Power sources*, Vol.158, 2006, pp.987-990.